Magnetic fluctuations and possible formation of a spin-singlet cluster under pressure in the heavy-fermion spinel LiV_2O_4 probed by ^{7}Li and ^{51}V NMR

Hikaru Takeda,[1,*] Yusuke Kato,[1] Masahiro Yoshimura,[1] Yasuhiro Shimizu,[1] Masayuki Itoh,[1]
Seiji Niitaka,[2] and Hidenori Takagi[3,4]

[1]*Department of Physics, Graduate School of Science, Nagoya University, Furo-cho, Chikusa-ku, Nagoya 464-8602, Japan*
[2]*RIKEN Advanced Science Institute, 2-1 Hirosawa, Wako, Saitama 351-0198, Japan*
[3]*Department of Physics, Graduate School of Science, University of Tokyo, 7-3-1 Hongo, Bunkyo-ku, Tokyo 113-0033, Japan*
[4]*Max Plank Institute for Solid State Research, Heisenbergstrasse 1, 70569 Stuttgart, Germany*

(Received 22 May 2015; published 6 July 2015)

^{7}Li and ^{51}V NMR measurements up to 9.8 GPa have been made to elucidate local magnetic properties of a heavy-fermion spinel oxide LiV_2O_4 which undergoes a metal-insulator transition above ∼7 GPa. The temperature T and pressure P dependences of the ^{7}Li and ^{51}V Knight shifts and the nuclear spin-lattice relaxation rates $1/T_1$ show that in the metallic phase, there is a crossover from a high-T region with weak ferromagnetic fluctuations to a low-T one with antiferromagnetic (AFM) fluctuations. The AFM fluctuations are enhanced below 20 K and 1.5 GPa, where a heavy Fermi-liquid state with the modified Korringa relation is formed. The evolution of the magnetic fluctuations is discussed from the aspect of the competition among several magnetic interactions. Above $P_{MI} \sim 6.7$ GPa, we find the coexistence of metallic and insulating phases due to the first-order metal-insulator transition. The ^{7}Li and ^{51}V NMR spectra coming from the insulating phase have T-independent small Knight shifts and $^7(1/T_1)$ with the thermally activated T dependence, indicating the formation of a spin-singlet cluster. We propose a model of a spin-singlet tetramer as discussed in geometrically frustrated materials.

DOI: 10.1103/PhysRevB.92.045103 PACS number(s): 71.27.+a, 71.30.+h, 76.60.−k

I. INTRODUCTION

Heavy Fermi liquid (HFL) is one of the most attractive phenomena in strongly correlated electron systems, since it is related to rich physics such as the Kondo effect, quantum criticality, or unconventional superconductivity in f electron systems [1–3]. In d electron systems, the HFL behavior appears in several materials with geometrically frustrated lattices [4–10]. Among them, a typical example is LiV_2O_4 with the spinel structure, where V ions form the frustrated pyrochlore lattice [11–17]. This d electron system is expected to have an anomalous HFL mechanism different from the Kondo effect that is well established in the f electron systems.

LiV_2O_4 with a formal valence of $V^{3.5+}$ ($3d^{1.5}$) behaves as a Fermi liquid (FL) having a large electronic specific-heat coefficient $\gamma \sim 420$ mJ/mol K^2 below 10 K [11]. The crossover from a high-temperature incoherent metal to a low-temperature FL was observed at ∼20 K by several probes such as resistivity [11,16], photoemission spectroscopy [18], and optical conductivity [19] measurements. Below the crossover temperature, an enhancement of antiferromagnetic (AFM) fluctuations was probed by nuclear magnetic resonance (NMR) [13,20–22] and inelastic neutron-scattering measurements [23–25]. There is no magnetic order down to 20 mK due to the magnetic frustration [11]. These experimental facts lead us to expect that the magnetic properties may be closely related to the HFL behavior, as discussed in theoretical studies based on the frustration effect [26–29].

The local electronic state of LiV_2O_4 has been discussed intensively to elucidate the mechanism of the HFL behavior. Implementations of the density functional theory in the local density approximation reveal that the t_{2g} orbital is split into degenerate e'_g and nondegenerate a_{1g} ones due to the local trigonal distortion, whereas the splitting is not large enough to separate these two bands [30–34]. Based on the band structure calculation, Anisimov *et al.* propose that the a_{1g} and e'_g bands have localized and itinerant characters, respectively, with different bandwidths, leading to the HFL behavior due to the Kondo effect [30]. Such a multiorbital effect can also cause the strong Hund coupling [35], interorbital Coulomb interaction [36], unconventional orbital fluctuations [37–39], or orbital selective Mott transition [40]. Furthermore, it is discussed that the geometrical spin frustrations [26–29], strong electron correlations [18,19], or one-dimensional spin fluctuation may also be related to the HFL behavior [41,42]. However, the mechanism of the HFL behavior remains unclear in spite of many experimental and theoretical studies.

Studies on pressure P effects can provide a root to reveal the peculiar feature associated with the HFL of LiV_2O_4. From the ^{7}Li nuclear spin-lattice relaxation rate $^7(1/T_1)$ measurement under pressure up to 4.7 GPa, it was proposed that the AFM fluctuations increase with increasing P and there is a quantum critical point (QCP) somewhere above 4.7 GPa [43,44]. Theoretical studies of $^7(1/T_1)$ based on the self-consistent renormalization (SCR) theory well reproduced the AFM fluctuations [45]. However, the presence of QCP has not been confirmed experimentally and the magnetic properties under pressure have not been well elucidated. Also electrical resistivity measurements under high pressure recently revealed that a metal-insulator transition (MIT) takes place above ∼7 GPa [46]. Subsequently, optical conductivity measurements up to 20 GPa with a diamond-anvil cell clarified that the metallic phase coexists with the insulating one above ∼6 GPa [47]. Furthermore, x-ray diffraction and extended x-ray absorption fine-structure (EXAFS) measurements observed a crystal structure change at the MIT, although the

*Present address: Institute for Solid State Physics, University of Tokyo, 5-1-5 Kashiwanoha, Kashiwa, Chiba 277-8581, Japan.

structure of the insulating phase has not been obtained [48–50]. An experimental study using a local probe such as NMR is useful for revealing magnetic and electronic properties of the insulating phase related to the MIT mechanism. However, no high-pressure NMR measurement on LiV_2O_4 above ∼5 GPa has been performed because of the technical difficulty of the accessibility of high pressures [51–53].

In this study, we have conducted ^{7}Li and ^{51}V NMR measurements on a powder sample up to 9.8 GPa to investigate local magnetic properties of LiV_2O_4. We present the temperature T and P dependences of the ^{7}Li and ^{51}V Knight shifts, ^7K and ^{51}K, and the nuclear spin-lattice relaxation rates, $^7(1/T_1)$ and $^{51}(1/T_1)$. Based on the experimental results, we find that a crossover takes place from the FL state with the AFM fluctuations to the less correlated metal where the magnetic fluctuations are suppressed with increasing P. Above $P_{\rm MI} \sim$ 6.7 GPa, i.e., the critical pressure where the MIT occurs at zero temperature, we observe the ^{7}Li and ^{51}V NMR spectra coming from both the metallic and insulating phases due to their coexistence. The latter spectra with T-independent small Knight shifts and the thermally activated $^7(1/T_1)$ show the presence of a nonmagnetic V site. We propose a spin-singlet tetramer model as the magnetic ground state in the insulating phase.

II. EXPERIMENTAL PROCEDURE

A powdered sample of LiV_2O_4 used in this study was prepared as described in Ref. [14]. ^{7}Li and ^{51}V NMR measurements were performed utilizing a coherent pulsed spectrometer and a superconducting magnet with a constant field $H = 6.105$ T. Fourier-transformed (FT) NMR spectra for spin-echo signals were measured. The ^{7}Li and ^{51}V Knight shifts were determined as $^{\mu}K = (\nu^{\mu}_{\rm res} - \nu^{\mu}_0)/\nu^{\mu}_0$ ($\mu = 7$ and 51) where $\nu^{\mu}_{\rm res}$ and ν^{μ}_0 (=101.023 MHz for ^{7}Li and 68.333 MHz for ^{51}V) are ^{7}Li and ^{51}V resonance frequencies in LiV_2O_4 and the aqueous $LiCl_2$ and $NaVO_3$ solution, respectively. The nuclear spin-lattice relaxation rates were measured by the saturation recovery method. The ^{7}Li and ^{51} V nuclear magnetizations after saturation pulses recovered single exponentially with T_1. $^{51}(1/T_1)$ could not be measured below ∼20 K, since we could not saturate the ^{51}V nuclear magnetization for the initial condition [13,20]. We used an opposed-anvil-type high-pressure cell, developed by Kitagawa *et al.* [53], with glycerol as a pressure medium. Pressure was monitored by measuring the ^{63}Cu nuclear quadrupole resonance frequency of a powdered Cu_2O at 300 K [53–55].

III. RESULTS AND ANALYSIS

A. Metallic phase

We first present ^{7}Li NMR results in the metallic phase of LiV_2O_4. Figure 1 shows the T dependences of the ^{7}Li NMR spectra, normalized by the intensity of its maximum peak. At ambient pressure, the single-peak spectrum shifts to a higher frequency and broadens upon cooling down to ∼20 K, as seen in Fig. 1(a). The linewidth depends on the impurity concentration [13], and the full width at half maximum (FWHM) of 0.11 MHz below ∼20 K corresponds to the ∼0.3 mol% impurity concentration which is quite small to affect the P effects on ^7K and $^7(1/T_1T)$. With increasing

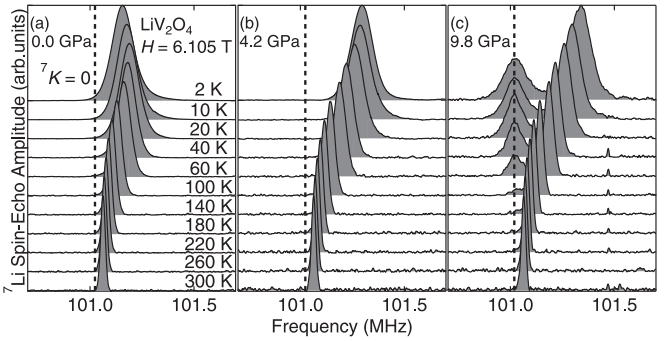

FIG. 1. Temperature dependences of the ^{7}Li NMR spectra in a magnetic field of $H = 6.105$ T at (a) ambient pressure, (b) 4.2, and (c) 9.8 GPa in LiV_2O_4. The spin-echo amplitude is normalized against the spectrum peak.

P up to 4.2 GPa, the spectrum exhibits a shift toward a higher frequency as seen in Fig. 1(b). Further application of P above $P_{\rm MI}$ induces another spectrum around $^7K \sim 0$, as seen in Fig. 1(c) where it appears below 260 K at 9.8 GPa.

In Fig. 2(a), we summarize the T dependences of ^7K at various pressures up to 9.8 GPa. Here, ^7K monitors magnetic susceptibility χ of LiV_2O_4 via a transferred hyperfine interaction. At ambient pressure, ^7K increases with decreasing T down to ∼30 K and shows a broad peak around 20 K, as reported in previous studies [13,20–22]. The peak further broadens up to ∼1.5 GPa, coinciding with the enhancement of ^7K below 20 K. Above 1.5 GPa, the peak disappears and ^7K monotonically increases down to 2 K. ^7K turns to be suppressed slightly above ∼7.8 GPa. Figure 2(b) shows the T dependences of $^7(1/T_1T)$ in the metallic phase up to 9.8 GPa. At ambient pressure, $^7(1/T_1T)$ increases with decreasing T down to ∼10 K, and then reaches a constant value of ∼2.5 s^{-1} K^{-1}, consistent with the previous results where $^7(1/T_1T)$ depends on the impurity concentration [13]. The concentration in the present sample is estimated as ∼0.3 mol%. In contrast to ^7K, $^7(1/T_1T)$ is almost

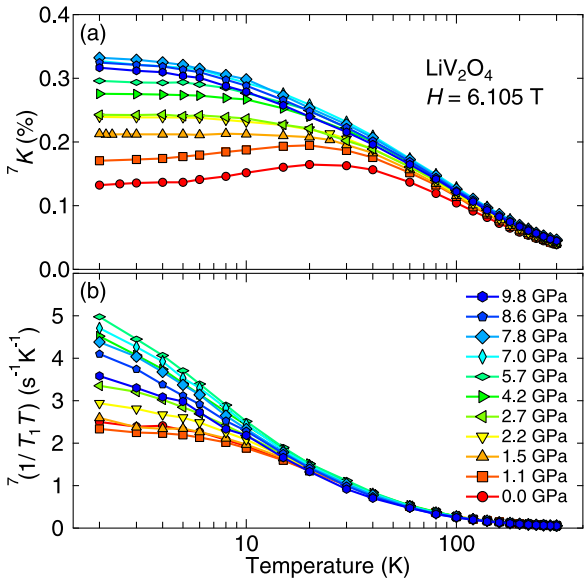

FIG. 2. (Color online) Temperature dependences of (a) ^7K and (b) $^7(1/T_1T)$ at various pressures up to 9.8 GPa in LiV_2O_4.

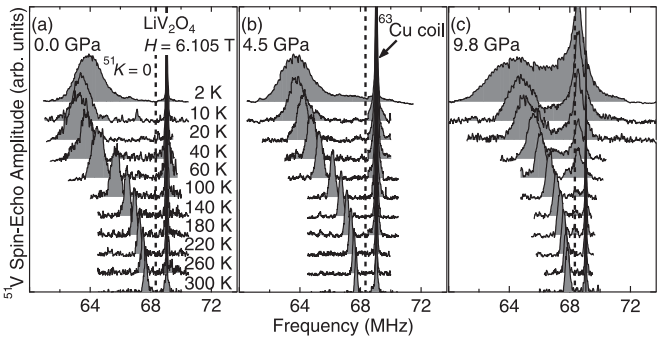

FIG. 3. Temperature dependences of the ^{51}V NMR spectra in a magnetic field of $H = 6.105$ T at (a) ambient pressure, (b) 4.5 GPa, and (c) 9.8 GPa in LiV_2O_4. The spin-echo amplitude is normalized against the maximum peak. The ^{63}Cu NMR spectrum comes from an NMR coil.

P independent below 1.5 GPa and increases in the P range of 1.5–5.7 GPa, but it becomes suppressed above 5.7 GPa.

Figure 3 shows the T dependences of the ^{51}V NMR spectra at ambient pressure, 4.2 GPa, and 9.8 GPa. The spectrum, which exhibits a negative Knight shift due to the core polarization effect, shifts toward a lower frequency with decreasing T at ambient pressure. It moves to a higher frequency with increasing P and another ^{51}V NMR spectrum appears near $^{51}K = 0$ at a low temperature below T_{MI}, as seen in Fig. 3(c) where it appears below ~200 K at 9.8 GPa. ^{51}K shows the T dependence similar to that of ^{7}K at each pressure, as seen in Fig. 4(a). However, it should be noted that the absolute value of ^{51}K is suppressed by P, inconsistent with ^{7}K. Figure 4(b) shows the T dependences of $^{51}(1/T_1T)$ at various pressures up to 9.8 GPa. Similar to $^{7}(1/T_1T)$, $^{51}(1/T_1T)$ in the observed P range monotonically increases with cooling down to 20 K, whereas it decreases with increasing P.

The P dependence of ^{51}K [$^{51}(1/T_1T)$] is different from that of ^{7}K [$^{7}(1/T_1T)$] as mentioned above. This is ascribed to the difference in the P dependence of the ^{51}V hyperfine

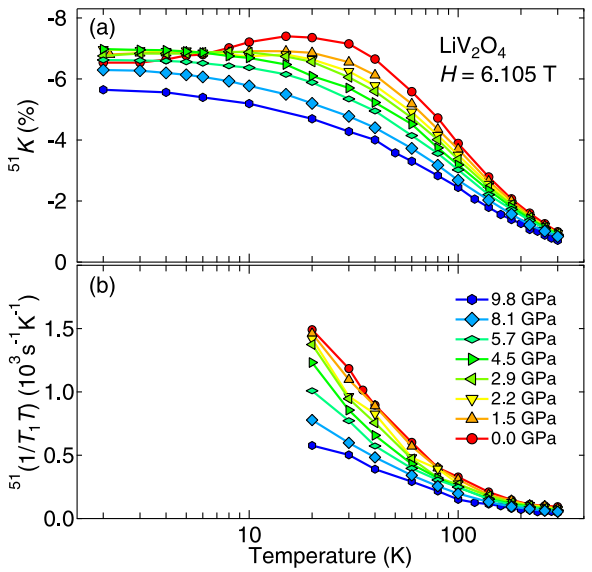

FIG. 4. (Color online) Temperature dependences of (a) ^{51}K and (b) $^{51}(1/T_1T)$ at various pressures up to 9.8 GPa in LiV_2O_4.

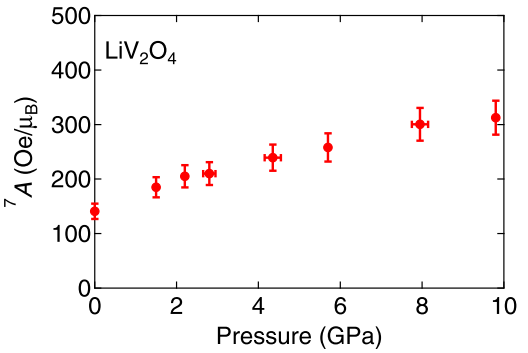

FIG. 5. (Color online) Pressure dependence of the ^{7}Li transferred hyperfine coupling constant ^{7}A in LiV_2O_4.

and the ^{7}Li transferred hyperfine coupling constants, ^{51}A and ^{7}A, respectively. The ^{7}Li nucleus has the isotropic transferred hyperfine interaction from the neighboring 12 V ions, leading to $^{7}K = 12 \times {}^{7}A\chi/N\mu_B$ with the Abogadro's number N and the Bohr magneton μ_B, while the ^{51}V nucleus interacts with the on-site $3d$ electrons via the hyperfine interaction. Then, ^{7}A is considered to become larger with increasing P because the V-O-Li bond length and the bond angle in the transferred path are sensitive to P, whereas ^{51}A is less sensitive to P. Assuming the P-independent ^{51}A (=−81 kOe/μ_B at ambient pressure [20]), we can evaluate the P dependence of ^{7}A from a relation $^{7}A = {}^{7}K{}^{51}A/(12 \times {}^{51}K)$ as shown in Fig. 5. This P dependence of ^{7}A also reasonably explains the difference between $^{7}(1/T_1T)$ and $^{51}(1/T_1T)$.

Next we extract the spin parts of K and $1/T_1T$ from the experimental results to study spin susceptibility. ^{51}K is generally expressed as $^{51}K = {}^{51}K_{spin}(T) + {}^{51}K_{orb}$, where $^{51}K_{spin}$ and $^{51}K_{orb}$ are the T-dependent spin and the T-independent Van Vleck orbital terms, respectively, and a small diamagnetic shift is ignored, whereas there is no orbital contribution to ^{7}K. We obtain $^{51}K_{orb}$ from the ^{51}K versus ^{7}K plots where the intercept of the fitted line provides a $^{51}K_{orb}$ value, as shown in Fig. 6(a). $^{51}K_{orb}$ reduces from 0.47 ± 0.08% at ambient pressure to 0.21 ± 0.08% at 9.8 GPa with increasing P. In Fig. 6(b), the T dependence of $^{51}K_{spin}$ is displayed after subtracting $^{51}K_{orb}$ from ^{51}K. Similar to the Knight shift, $^{51}(1/T_1T)$ is composed of the spin and orbital terms as $^{51}(1/T_1T) = {}^{51}(1/T_1T)_{spin} + {}^{51}(1/T_1T)_{orb}$. The orbital term

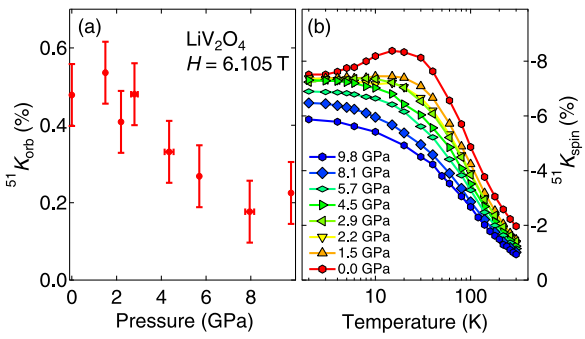

FIG. 6. (Color online) (a) Pressure dependence of the ^{51}V orbital Knight shift $^{51}K_{orb}$ in LiV_2O_4. (b) Temperature dependences of the ^{51}V Knight shift due to spin susceptibility $^{51}K_{spin}$ at various pressures.

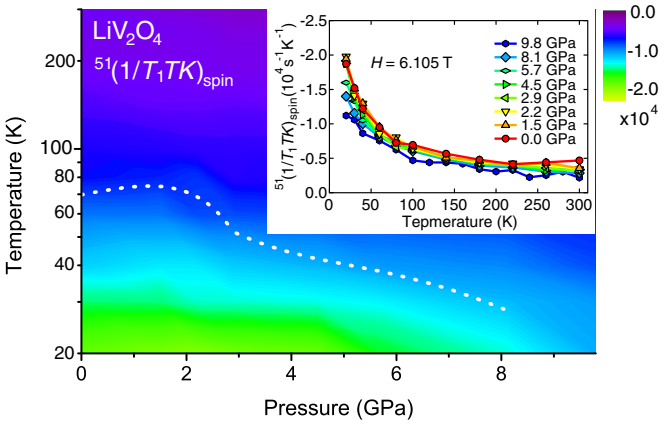

FIG. 7. (Color online) Contour plot of pressure and temperature dependences of $^{51}(1/T_1TK)_{\rm spin}$ in LiV_2O_4. Inset: The temperature dependences of $^{51}(1/T_1TK)_{\rm spin}$ at several pressures. The dashed curve represents the pressure dependence of the onset temperature $T_{\rm co}$ at which the absolute value of the T derivative of $^{51}(1/T_1TK)_{\rm spin}$ starts to increase with decreasing T.

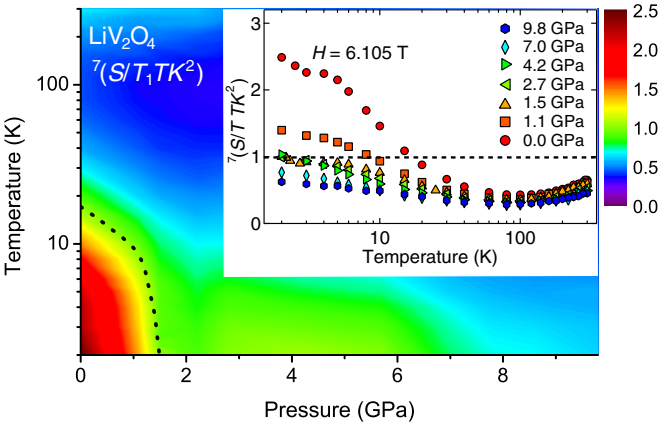

FIG. 8. (Color online) Contour plot of pressure and temperature dependences of $^{7}(S/T_1TK^2)$, where $S = \frac{\hbar}{4\pi k_{\rm B}}(\frac{\gamma_{\rm e}}{\gamma_{\rm n}})^2$, in LiV_2O_4. Inset: The temperature dependences of $^{7}(S/T_1TK^2)$ at several pressures. On the dashed curve, $^{7}(S/T_1TK^2) = 1$.

can be obtained from the $^{51}(1/T_1T)$ versus $^{7}(1/T_1T)$ plots where $^{7}(1/T_1T)$ is governed by the spin fluctuation, namely, $^{7}(1/T_1T) = {}^{7}(1/T_1T)_{\rm spin}$. We found almost P-independent $^{51}(1/T_1T)_{\rm orb}$ ($=25 \pm 5$ s^{-1} K^{-1} obtained at ambient pressure) much less than $^{51}(1/T_1T)_{\rm spin}$, as seen in Fig. 4(b).

Based on the above results, we can obtain information on the T and P dependences of static spin susceptibility $\chi(0,0)$ from the Knight shifts and dynamical spin susceptibility $\chi(\mathbf{q},\omega)$ from $1/T_1T$. At ambient pressure, ^{7}K and ^{51}K saturate at low temperatures below 20 K, whereas $^{7}(1/T_1T)$ and $^{51}(1/T_1T)$ increase with decreasing T. This shows that the AFM fluctuations develop at low temperatures, as discussed in our previous study [20], consistent with the development of the inelastic peak at the wave number $q \sim 0.6$ Å^{-1} observed below 40 K in the neutron-scattering experiments [23–25]. Below 6 K, both ^{7}K and $^{7}(1/T_1T)$ become almost T independent as expected in the FL, although $^{7}(1/T_1T)$ slightly increases towards 2 K due to the impurity effect [13]. With applying P, the T-independent behavior of ^{7}K, ^{51}K, and $^{7}(1/T_1T)$ rapidly disappears around ~1.5 GPa. Furthermore, ^{51}K and $^{51}(1/T_1T)$ reduce with increasing P above ~1.5 GPa, showing the suppression of both $\chi(0,0)$ and $\chi(\mathbf{q},\omega)$.

To illustrate these characteristic behaviors of the magnetic fluctuations in the P-T phase diagram, we present two contour plots comparing $\chi(0,0)$ with $\chi(\mathbf{q},\omega)$. One is Fig. 7, which shows the T and P dependences of $^{51}(1/T_1TK)_{\rm spin}$ monitoring the magnetic fluctuations via a relation $^{51}(1/T_1TK)_{\rm spin} \propto \sum_{\mathbf{q}} {\rm Im}\chi_{\perp}(\mathbf{q},\omega_{\rm n})/\chi(0,0)$, with $\chi_{\perp}(\mathbf{q},\omega)$ the transverse component of $\chi(\mathbf{q},\omega)$ and the NMR frequency $\omega_{\rm n}$ [56]. This plot is useful for revealing the ratio of the $q \neq 0$ component to the uniform one in the magnetic fluctuations. The almost T-independent behavior of $^{51}(1/T_1TK)_{\rm spin}$ above ~200 K indicates the dominant ferromagnetic (FM) fluctuations. We can also see that the fraction of the $q \neq 0$ component gradually increases with decreasing T and is more enhanced below a temperature $T_{\rm co}$ (~70 K at ambient pressure) which gradually decreases with increasing P, as seen in Fig. 7. Here the dashed curve in Fig. 7 represents the P dependence of the onset temperature $T_{\rm co}$ at which the absolute value of the T derivative of $^{51}(1/T_1TK)_{\rm spin}$ starts to increase with decreasing T. Thus the magnetic fluctuations show a crossover from the high-T ferromagnetic (FM) to low-T AFM fluctuations. To clarify the character of the magnetic fluctuations below ~20 K, the ^{7}Li data are valuable, but the P effect on ^{7}A prevents us from obtaining the P dependence of the magnetic fluctuations from $^{7}(1/T_1TK)$. For removing this P effect, we present another plot in Fig. 8, which shows the T and P dependences of $^{7}(S/T_1TK^2)$ where S is a normalization factor expressed as $S=\frac{\hbar}{4\pi k_{\rm B}}(\frac{\gamma_{\rm e}}{\gamma_{\rm n}})^2$ with the Planck's constant $\hbar$, the Boltzman factor $k_{\rm B}$, and the nuclear (electron) gyromagnetic ratio $\gamma_{\rm n}$ ($\gamma_{\rm e}$). Here S is introduced to discuss the Korringa parameter $^{7}K(\alpha)$ in Sec. IV A. $^{7}(S/T_1TK^2)$ can monitor the magnetic fluctuations via a relation $^{7}(1/T_1TK^2) \propto \sum_{\mathbf{q}} F(\mathbf{q}){\rm Im}\chi_{\perp}(\mathbf{q},\omega_{\rm n})/\chi(0,0)^2$ with a form factor of the transferred hyperfine interaction $F(\mathbf{q})$ [57]. In this plot, the P effect on ^{7}A is removed. As seen in Fig. 8, there is a region where $^{7}(S/T_1TK^2)$ is strongly enhanced inside the dotted curve on which $^{7}(S/T_1TK^2) = 1$. Outside this region, $^{7}(S/T_1TK^2)$ reduces with increasing P at low temperatures, corresponding to the suppression of $\chi(0,0)$ and $\chi(\mathbf{q},\omega)$. Also, below 70 K, $^{7}(S/T_1TK^2)$ turns to increase with decreasing T, consistent with the enhancement of the $q \neq 0$ component mentioned above.

B. Insulating phase

Above $P_{\rm MI}$, we observed the ^{7}Li and ^{51}V NMR spectra with the small ^{7}K and ^{51}K as mentioned above. The P dependence of the onset temperature $T_{\rm MI}$, below which the spectra appear, is presented in Fig. 9(a), where the phase boundaries determined by the optical conductivity measurement under high pressure are shown for comparison [47]. The $P_{\rm MI}$ value of 6.7 GPa in the present sample is determined by extrapolating the P dependence of $T_{\rm MI}$ to zero temperature. The optical conductivity measurement demonstrates an intermediate region in the P range of 6–10 GPa, where the metallic and insulating phases coexist. Thus the nonmagnetic NMR spectra are considered to come from the ^{7}Li and ^{51}V nuclei in the insulating domains

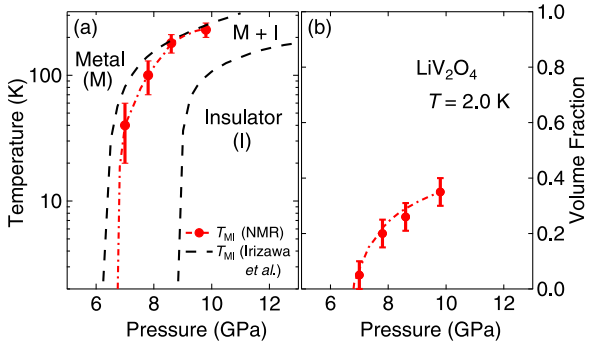

FIG. 9. (Color online) (a) Pressure dependence of the onset temperature T_{MI} below which the ^{7}Li NMR spectrum coming from the insulating phase appears in LiV_2O_4. (b) Pressure dependence of the volume fraction of the ^{7}Li NMR spectrum at 2.0 K in LiV_2O_4. The broken curves are the metal-insulator transition boundaries determined by the optical conductivity measurement (Ref. [47]) which observed the intermediate phase between the metallic and insulating phases. The dot-dashed curves are guides to the eye.

of the sample. Observation of both the metallic and insulating NMR spectra clearly shows the coexistence of both phases, consistent with a first-order MIT, which accompanies the structural transition observed by optical conductivity [47], x-ray [48], and EXAFS [49,50] measurements.

The volume fraction of the insulating phase is obtained from the ratio between the integrated intensities of the metallic and insulating NMR spectra after the T_2 correction. The P dependence of the fraction in the ^{7}Li NMR spectrum at 2.0 K is presented in Fig. 9(b). The fraction increases with increasing P but does not reach 100% even at 9.8 GPa. Although similar behavior was observed for the ^{51}V NMR spectra in the intermediate region, the powdered patterns with a fast and anisotropic T_2 from the metallic phase hardly evaluate the volume fraction.

The T dependences of ^7K, ^{51}K, and $^7(1/T_1)$ in the insulating phase at 9.8 GPa are presented with the Knight

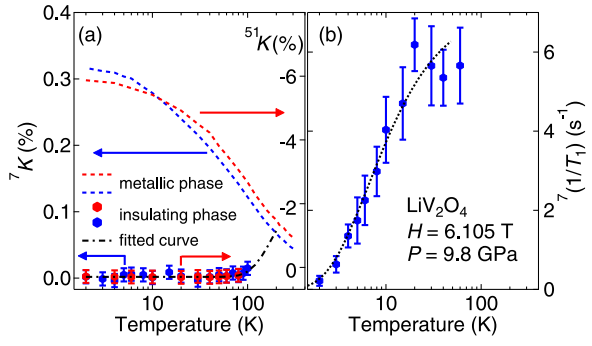

FIG. 10. (Color online) Temperature dependences of (a) ^7K (solid blue hexagon), ^{51}K (solid red hexagon), and (b) $^7(1/T_1)$ at 9.8 GPa in the insulating phase of LiV_2O_4. The ^7K (blue dashed curve) and ^{51}K (red dashed curve) data in the metallic phase are presented for comparison. The dot-dashed curve in the left panel is the fitted result of ^{51}K with a singlet-triplet model having a gap energy of 590 K, whereas the dotted curve in the right panel is the fitted result, $^7(1/T_1) = a\exp(-\Delta/k_BT)$ with $a = 7.2$ s^{-1} and $\Delta = 6.6$ K.

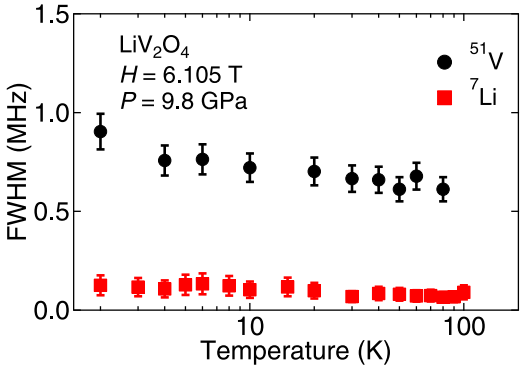

FIG. 11. (Color online) Temperature dependences of the full width at half maximum (FWHM) of the insulating ^{7}Li and ^{51}V NMR spectra at 9.8 GPa in LiV_2O_4.

shifts of the metallic phase in Fig. 10. Both the Knight shifts in the insulating phase, $^7K = 0.005 \pm 0.003\%$ and $^{51}K = 0.29 \pm 0.03\%$, are small and independent of T, as seen in Fig. 10(a), indicating the presence of a nonmagnetic V site. The small ^7K is a chemical shift, whereas the ^{51}K is not a chemical shift of V^{5+} but comparable to the Van Vleck orbital shifts of nonmagnetic clusters, for example, 0.35% in a trimer composed of V^{3+} in $LiVO_2$ [58]. The presence of the nonmagnetic V site is also confirmed by $^7(1/T_1)$, which obeys the thermally activated T dependence $^7(1/T_1) = a\exp(-\Delta/k_BT)$ with $a = 7.2 \pm 0.5$ s^{-1} and $\Delta = 6.6 \pm 0.7$ K, as represented by the dotted curve in Fig. 10(b). Also ^{51}K can be reproduced in a simple singlet-triplet model, $^{51}K = K_0 + K_1/\{1 + \frac{1}{3}\exp(\Delta/k_BT)\}$ with $K_0 = 0.30 \pm 0.03\%$, $K_1 = -2200 \pm 500$, and $\Delta = 590 \pm 20$ K, as seen in Fig. 10(a). These results mean that the nonmagnetic V site has a magnetic excited state composed of a small (large) gap energy at $q \neq 0$ ($q = 0$) over the nonmagnetic ground state. It is also noted that no broadening in the Li and V NMR spectra shows the absence of a long-range magnetic order in the insulating phase of LiV_2O_4, as seen in Fig. 11.

IV. DISCUSSION

A. Magnetic fluctuations in the metallic phase

Based on the NMR experimental results, we discuss the P effect on the magnetic fluctuations and propose a schematic P-T phase diagram in Fig. 12. The MIT takes place above P_{MI} where the metallic and insulating phases coexist up to the measured maximum pressure of 9.8 GPa, as denoted by the dot-dashed curve in Fig. 12. In the metallic phase, there is a crossover from a high-T region with the weak FM fluctuations to a low-T region with the AFM ones, as represented by the dashed curve, which is a rough guide to the eye. Furthermore, there is a region with the enhanced $^7(S/T_1TK^2)$ below ~20 K and ~1.5 GPa, as depicted in Fig. 8. Inside this region, we observed the T-independent ^7K and $^7(1/T_1T)$ which are evidence of the FL state following the modified Korringa relation with a parameter $K(\alpha) = S/T_1TK^2$. It provides a measure of the magnetic fluctuations, namely, $K(\alpha) < 1$ for the FM fluctuations and $K(\alpha) > 1$ for the AFM fluctuations [59,60]. As seen in Fig. 8, the value of $^7(S/T_1TK^2)$ corresponding to $^7K(\alpha)$ over unity means

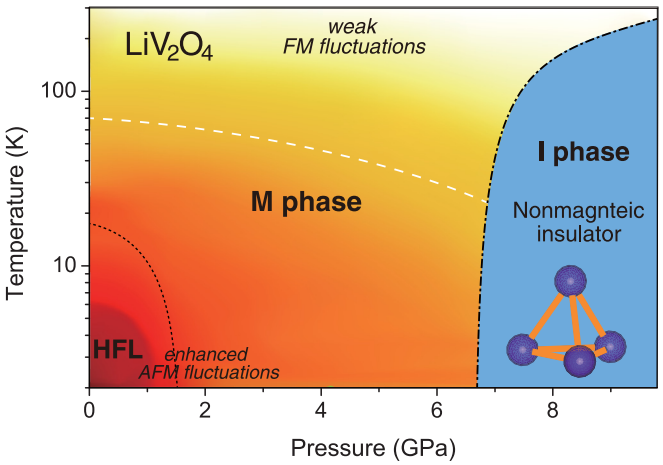

FIG. 12. (Color online) Schematic pressure vs temperature phase diagram in LiV_2O_4. The dot-dashed curve represents the metal-insulator transition boundary above which the insulating (I) phase appears with the coexistent metallic (M) phase. In the metallic phase, the dashed curve is a crossover temperature below which the antiferromagnetic (AFM) fluctuations develop with decreasing T, whereas the dotted curve is another one around which a crossover takes place with increasing T and P from a heavy Fermi liquid (HFL) to a correlated metal, with the AFM fluctuations whose intensity is schematically denoted by the color gradation. The insulating phase is nonmagnetic due to a possible formation of a spin-singlet V tetramer.

that the FL state with the AFM fluctuations is stabilized particularly below ∼6 K. The system rapidly ceases to follow the Korringa relation with applying P. With further increasing P above ∼1.5 GPa, both the $q = 0$ and $q \neq 0$ components of the magnetic fluctuations are suppressed and, particularly, the $q \neq 0$ one reduces in comparison with $q = 0$. Thus, around the boundary in which $^7K(\alpha) > 1$, denoted by the dotted curve in Fig. 12, a crossover takes place from the HFL state with the AFM fluctuations to a correlated metallic state where the AFM ones reduce with increasing P, as represented by the color gradation in Fig. 12. With further applying P, the system is considered to approach a Pauli paramagnet with suppressed electron correlation, although the MIT takes place before entering into such a state. Thus the HFL behavior is concluded to appear in the region with the most enhanced AFM fluctuations. However, it should be noted that the magnetic fluctuations have no critical behavior in the P-T phase diagram. This fact excludes the presence of QCP at ambient pressure, even if it may be located in the vicinity of QCP by the Zn doping to LiV_2O_4 [9,61]. The suppression of the magnetic fluctuations above 1.5 GPa also shows the absence of the magnetic QCP somewhere above ∼4.7 GPa predicted on the basis of the previous ^{7}Li NMR results [44,45].

From the theoretical point of view, the magnetic properties of LiV_2O_4 have been discussed from two different approaches, starting with the strong- and weak-coupling limits for the electron correlation. In the weak-coupling approach, the spin susceptibility is described within the random phase approximation, demonstrating a multipeak structure of generalized susceptibility $\chi(q)$ due to the geometrical frustration, where the $\chi(q)$ peaks are enhanced by the electron correlation, in the **q** space [38,62]. Application of pressure reasonably reduces the effective electron correlation via increasing the bandwidth, and therefore is expected to qualitatively decrease the magnetic fluctuations. Then this might explain the drastic suppression of the AFM fluctuations observed above ∼1.5 GPa, if the frustration is removed at the crossover pressure. On the other hand, the strong-coupling approach may provide a scenario for the pressure effect as follows. The magnetic properties have been discussed on the basis of the effective Hamiltonians constructed from the unique band structure with the e'_g and a_{1g} bands which have itinerant and localized characters, respectively [30]. There are several competitive magnetic interactions, such as AFM superexchange interactions in the a_{1g} spins, FM double-exchange interactions via the e'_g electron hopping, and Kondo exchange interactions between the a_{1g} and e'_g spins [26–29,35,37]. In LiV_2O_4 with the pyrochlore lattice, the geometrical frustration plays an important role in the absence of magnetic order. Focusing on the a_{1g} spins, the system is regarded as a spin liquid with short-range AFM correlations due to the geometrical frustration [20,26–29,37]. The e'_g electrons coupled with the a_{1g} spins through the Hund exchange coupling effectively reduce the AFM correlations via the transfer hopping process [28,29,35,37]. Under pressure, the e'_g bandwidth is reasonably expected to become broader than the a_{1g} band due to transfer paths to the neighboring sites, leading to the FM double-exchange interaction more effectively enhanced than the AFM superexchange interaction. Thus, the competition among several magnetic interactions may suppress the AFM fluctuations at high pressures above ∼1.5 GPa; then the spin-liquid entropy contributing the effective mass of the e'_g conduction electrons becomes suppressed [20,26–29]. This possible scenario may provide significant insight into the mechanism of the HFL behavior in LiV_2O_4.

B. Nonmagnetic state in the insulating phase

We focus on the magnetic properties of the insulating phase above P_{MI} (Fig. 12). In geometrically frustrated systems with charge and/or orbital degrees of freedom, the frustration is often removed by forming a spin-singlet cluster such as a trimer ($LiVO_2$) [58,63,64], heptermer (AlV_2O_4) [65–67], helical dimer ($MgTi_2O_4$) [68], or octamer ($CuIr_2S_4$) [69] with charge and/or orbital orders accompanied by a structural transition. The nonmagnetic vanadium site in the insulating phase of LiV_2O_4 elucidates such formation of a spin-singlet cluster. In fact, the local lattice distortion along [111] on the pseudocubic lattice observed by the EXAFS experiment below T_{MI} in LiV_2O_4 is similar to that in AlV_2O_4 where a nonmagnetic V heptamer and a magnetic V^{4+} site are formed [50], although the lack of detailed data of the crystal structure prevents us from discussing the spin-singlet cluster from the structural point of view in the insulating phase of LiV_2O_4.

There are two possible scenarios to explain the presence of the nonmagnetic state observed in the present NMR experiment on LiV_2O_4 by taking account of the tetrahedral unit with six 3d spins. The spinel or pyrochlore structure viewed from the [111] direction has the alternative stacking of triangular and kagome lattices. One scenario is the coexistence of a nonmagnetic V^{5+} site on the triangular lattice and a nonmagnetic trimer formed by V^{3+}, where six 3d electrons

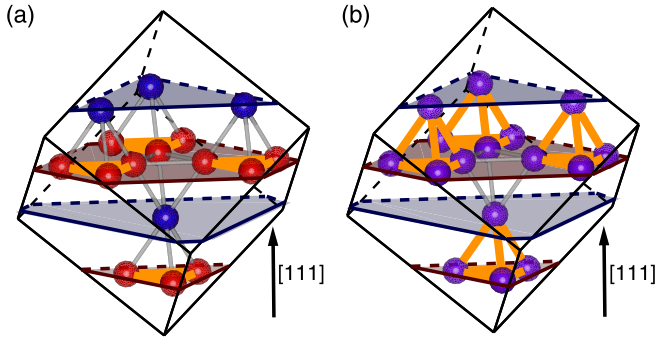

FIG. 13. (Color online) Schematic illustration of (a) V trimer spin-singlet clusters (triangles with orange bonds and red spheres) and (b) tetramer spin-singlet clusters (tetrahedra with orange bonds and purple spheres) in a pseudocubic unit cell of the spinel structure proposed in the insulating phase of LiV_2O_4. The blue and red spheres denote the V^{5+} and V^{3+} ions, respectively.

occupy bonding molecular orbitals, on the kagome lattice, as shown in Fig. 13(a). However, the coexistence of V^{3+} and V^{5+} sites is quite unusual and it may also be ruled out since we observed only a kind of nonmagnetic ^{51}V and ^{7}Li NMR spectra. Another scenario is the formation of a V-tetramer singlet cluster, as presented in Fig. 13(b). A V-tetrahedron sharing six $3d$ electrons can have 12 molecular orbitals formed by the t_{2g} orbitals and they split to five multiplets in a cubic symmetry [37]. While the moderate Hund coupling can partly polarize spins of the tetrahedron in the cubic symmetry [37], the lowering of the crystal symmetry is expected to induce the further orbital splitting, which may make a low-spin electron configuration, resulting in the nonmagnetic tetramer, stable to release the spin frustration in the insulating phase. Then the tetramer may have a magnetic excited state having the large dispersion with a small (large) gap energy at $q \neq 0$ ($q = 0$) as observed in the present NMR measurements. Thus, LiV_2O_4 would exhibit the structural transition accompanied by the MIT to form the tetramer singlet as observed in some chromium oxides with the breathing pyrochlore lattice [70]. More recently, even in the metallic phase, electron delocalization in the tetrahedron unit was revealed to play a crucial role for the magnetic fluctuations [25]. The competition and/or cooperation among spin, orbital, and charge degrees of freedom in the tetrahedron unit may govern the peculiar magnetic properties of LiV_2O_4.

V. CONCLUSION

We have performed ^{7}Li and ^{51}V NMR measurements on a powder sample up to 9.8 GPa to elucidate the local magnetic properties of LiV_2O_4 which undergoes the metal-insulator transition above ∼7 GPa. Based on the temperature and pressure dependences of the Knight shifts and the nuclear spin-lattice relaxation rates, we found in the metallic phase a crossover below ∼70 K where the antiferromagnetic fluctuations develop with decreasing temperature. Furthermore, in a narrow region below ∼20 K and ∼1.5 GPa, another crossover was observed to take place from the correlated metallic state to the Fermi-liquid state with the enhanced antiferromagnetic fluctuations. Thus the HFL behavior was concluded to appear in the region with the most enhanced AFM fluctuations. This characteristic behavior of the magnetic fluctuations was discussed on the basis of the competition among the magnetic interactions due to the geometrical frustration. Above $P_{MI} \sim$ 6.7 GPa, in addition to the NMR spectra of the metallic phase, we observed the ^{7}Li and ^{51}V NMR spectra with the small Knight shifts coming from the insulating phase. We proposed the presence of a nonmagnetic V cluster forming a tetramer singlet.

ACKNOWLEDGMENTS

The authors would like to thank K. Kitagawa, S. Inoue, and K. Matsushita for technical advice about high-pressure cells and Y. Motome, T. Takimoto, and Y. Kobayashi for fruitful discussions. This study was supported by the Grant-in-Aid for Scientific Research, KAKENHI, on Priority Area "Novel State of Matter Induced by Frustration" (Grant No. 22014006) from the Ministry of Education, Culture, Sports, Science, and Technology of Japan, and also the Grants-in-Aid for Scientific Research, KAKENHI, (Grants No. 23225005 and No. 24340080) from the Japan Society for the Promotion of Science (JSPS). H.T. was also supported by the Program for Leading Graduate Schools entitled "Integrative Graduate Education and Research Program in Green Natural Sciences" and the Grant-in-Aid for JSPS Fellows.

[1] G. R. Stewart, Rev. Mod. Phys. **73**, 797 (2001).
[2] H. V. Löhneysen, A. Rosch, M. Vojta, and P. Wölfle, Rev. Mod. Phys. **79**, 1015 (2007).
[3] P. Gegenwart, Q. Si, and F. Steglich, Nat. Phys. **4**, 186 (2008).
[4] H. Wada, H. Nakamura, E. Fukami, K. Yoshimura, M. Shiga, and Y. Nakamura, J. Magn. Magn. Mater. **70**, 17 (1987).
[5] T. Shinkoda, K. Kumagai, and K. Asanuma, J. Phys. Soc. Jpn. **46**, 1754 (1979).
[6] K. Miyoshi, E. Morikuni, K. Fujiwara, J. Takeuchi, and T. Hamasaki, Phys. Rev. B **69**, 132412 (2004).
[7] Y. Okamoto, T. Shimizu, J. Yamakura, Y. Kiuchi, and Z. Hiroi, J. Phys. Soc. Jpn. **79**, 093712 (2010).
[8] H.-A. Krug von Nidda, R. Bulla, N. Büttgen, M. Heinrich, and A. Loidl, Eur. Phys. J. B **34**, 399 (2003).
[9] N. Büttgen, H.-A. Krug von Nidda, W. Kraetschmer, A. Günther, S. Widmann, S. Riegg, A. Krimmel, and A. Loidl, J. Low Temp. Phys. **161**, 148 (2010).
[10] C. Lacroix, J. Phys. Soc. Jpn. **79**, 011008 (2010), and references therein.
[11] S. Kondo, D. C. Johnston, C. A. Swenson, F. Borsa, A. V. Mahajan, L. L. Miller, T. Gu, A. I. Goldman, M. B. Maple, D. A. Gajewski, E. J. Freeman, N. R. Dilley, R. P. Dickey, J. Merrin, K. Kojima, G. M. Luke, Y. J. Uemura, O. Chmaissem, and J. D. Jorgensen, Phys. Rev. Lett. **78**, 3729 (1997).
[12] O. Chmaissem, J. D. Jorgensen, S. Kondo, and D. C. Johnston, Phys. Rev. Lett. **79**, 4866 (1997).
[13] A. V. Mahajan, R. Sala, E. Lee, F. Borsa, S. Kondo, and D. C. Johnston, Phys. Rev. B **57**, 8890 (1998).

[14] S. Kondo, D. C. Johnston, and L. L. Miller, Phys. Rev. B **59**, 2609 (1999).

[15] D. C. Johnston, C. A. Swenson, and S. Kondo, Phys. Rev. B **59**, 2627 (1999).

[16] C. Urano, M. Nohara, S. Kondo, F. Sakai, H. Takagi, T. Shiraki, and T. Okubo, Phys. Rev. Lett. **85**, 1052 (2000).

[17] Y. Matsushita, H. Ueda, and Y. Ueda, Nat. Mater. **4**, 845 (2005).

[18] A. Shimoyamada, S. Tsuda, K. Ishizaka, T. Kiss, T. Shimojima, T. Togashi, S. Watanabe, C. Q. Zhang, C. T. Chen, Y. Matsushita, H. Ueda, Y. Ueda, and S. Shin, Phys. Rev. Lett. **96**, 026403 (2006).

[19] P. E. Jonsson, K. Takenaka, S. Niitaka, T. Sasagawa, S. Sugai, and H. Takagi, Phys. Rev. Lett. **99**, 167402 (2007).

[20] Y. Shimizu, H. Takeda, M. Tanaka, M. Itoh, S. Niitaka, and H. Takagi, Nat. Commun. **3**, 981 (2012).

[21] M. Onoda, H. Imai, Y. Amako, and H. Nagasawa, Phys. Rev. B **56**, 3760 (1997).

[22] N. Fujiwara, H. Yasuoka, and Y. Ueda, Phys. Rev. B **57**, 3539 (1998).

[23] A. Krimmel, A. Loidl, M. Klemm, S. Horn, and H. Schober, Phys. Rev. Lett. **82**, 2919 (1999).

[24] S. H. Lee, Y. Qiu, C. Broholm, Y. Ueda, and J. J. Rush, Phys. Rev. Lett. **86**, 5554 (2001).

[25] K. Tomiyasu, K. Iwasa, H. Ueda, S. Niitaka, H. Takagi, S. Ohira-Kawamura, T. Kikuchi, Y. Inamura, K. Nakajima, and K. Yamada, Phys. Rev. Lett. **113**, 236402 (2014).

[26] C. Lacroix, Can. J. Phys. **79**, 1469 (2001).

[27] J. Hopkinson and P. Coleman, Phys. Rev. Lett. **89**, 267201 (2002).

[28] S. Burdin, D. R. Grempel, and A. Georges, Phys. Rev. B **66**, 045111 (2002).

[29] M. S. Laad, L. Craco, and E. Muller-Hartmann, Phys. Rev. B **67**, 033105 (2003).

[30] V. I. Anisimov, M. A. Korotin, M. Zolfl, T. Pruschke, K. Le Hur, and T. M. Rice, Phys. Rev. Lett. **83**, 364 (1999).

[31] V. Eyert, K. H. Hock, S. Horn, A. Loidl, and P. S. Riseborough, Europhys. Lett. **46**, 762 (1999).

[32] D. J. Singh, P. Blaha, K. Schwarz, and I. I. Mazin, Phys. Rev. B **60**, 16359 (1999).

[33] J. Matsuno, A. Fujimori, and L. F. Mattheiss, Phys. Rev. B **60**, 1607 (1999).

[34] I. A. Nekrasov, Z. V. Pchelkina, G. Keller, T. Pruschke, K. Held, A. Krimmel, D. Vollhardt, and V. I. Anisimov, Phys. Rev. B **67**, 085111 (2003).

[35] K. Le Hur, Phys. Rev. B **75**, 014435 (2007).

[36] H. Kusunose, S. Yotsuhashi, and K. Miyake, Phys. Rev. B **62**, 4403 (2000).

[37] K. Hattori and H. Tsunetsugu, Phys. Rev. B **79**, 035115 (2009).

[38] H. Tsunetsugu, J. Phys. Soc. Jpn. **71**, 1844 (2002).

[39] Y. Yamashita and K. Ueda, Phys. Rev. B **67**, 195107 (2003).

[40] R. Arita, K. Held, A. V. Lukoyanov, and V. I. Anisimov, Phys. Rev. Lett. **98**, 166402 (2007).

[41] S. Fujimoto, Phys. Rev. B **65**, 155108 (2002).

[42] R. Kadono, A. Koda, W. Higemoto, K. Ohishi, H. Ueda, C. Urano, S. Kondo, M. Nohara, and H. Takagi, J. Phys. Soc. Jpn. **81**, 014709 (2012).

[43] K. Fujiwara, H. Yoshioka, K. Miyoshi, J. Takeuchi, T. C. Kobayashi, and K. Amaya, Physica B **312**, 913 (2002).

[44] K. Fujiwara, K. Miyoshi, J. Takeuchi, Y. Shimaoka, and T. Kobayashi, J. Phys.: Condens. Matter **16**, S615 (2004).

[45] V. Yushankhai, T. Takimoto, and P. Thalmeier, J. Phys.: Condens. Matter **20**, 465221 (2008).

[46] C. Urano, Ph.D. thesis, The University of Tokyo, 2000.

[47] A. Irizawa, S. Suga, G. Isoyama, K. Shimai, K. Sato, K. Iizuka, T. Nanba, A. Higashiya, S. Niitaka, and H. Takagi, Phys. Rev. B **84**, 235116 (2011).

[48] K. Takeda, H. Hidaka, H. Kotegawa, T. C. Kobayashi, K. Shimizu, H. Harima, K. Fujiwara, K. Miyoshi, J. Takeuchi, Y. Ohishi, T. Adachi, M. Takata, E. Nishibori, M. Sakata, T. Watanuki, and O. Shimomura, Physica B **359**, 1312 (2005).

[49] N. Dragoe, L. Pinsard-Gaudart, J. P. Itie, A. Congeduti, P. Roy, S. Niitaka, H. Takagi, P. Lagarde, and A. M. Flank, High Press. Res. **26**, 427 (2006).

[50] L. Pinsard-Gaudart, N. Dragoe, P. Lagarde, A. M. Flank, J. P. Itie, A. Congeduti, P. Roy, S. Niitaka, and H. Takagi, Phys. Rev. B **76**, 045119 (2007).

[51] T. Suzuki, I. Yamauchi, Y. Shimizu, M. Itoh, N. Takeshita, C. Terakura, H. Takagi, Y. Tokura, T. Yamauchi, and Y. Ueda, Phys. Rev. B **79**, 081101(R) (2009).

[52] M. Itoh, JPSJ News Comments **7**, 03 (2010).

[53] K. Kitagawa, H. Gotou, T. Yagi, A. Yamada, T. Matsumoto, Y. Uwatoko, and M. Takigawa, J. Phys. Soc. Jpn. **79**, 024001 (2010).

[54] A. P. Reyes, E. T. Ahrens, R. H. Heffner, P. C. Hammel, and J. D. Thompson, Rev. Sci. Instrum. **63**, 3120 (1992).

[55] H. Fukazawa, N. Yamatoji, Y. Kohori, C. Terakura, N. Takeshita, Y. Tokura, and H. Takagi, Rev. Sci. Instrum. **78**, 015106 (2007).

[56] T. Moriya, Prog. Theor. Phys. **28**, 371 (1962).

[57] F. Mila and T. M. Rice, Phys. Rev. B **40**, 11382 (1989).

[58] T. Jin-no, Y. Shimizu, M. Itoh, S. Niitaka, and H. Takagi, Phys. Rev. B **87**, 075135 (2013).

[59] T. Moriya, J. Phys. Soc. Jpn. **18**, 516 (1963).

[60] A. Narath and H. T. Weaver, Phys. Rev. **175**, 33 (1968).

[61] Y. Ueda, N. Fujiwara, and H. Yasuoka, J. Phys. Soc. Jpn. **66**, 778 (1997).

[62] V. Yushankhai, A. Yaresko, P. Fulde, and P. Thalmeier, Phys. Rev. B **76**, 085111 (2007).

[63] J. B. Goodenough, G. Dutta, and A. Manthiram, Phys. Rev. B **43**, 10170 (1991).

[64] H. F. Pen, J. van den Brink, D. I. Khomskii, and G. A. Sawatzky, Phys. Rev. Lett. **78**, 1323 (1997).

[65] K. Matsuno, T. Katsufuji, S. Mori, Y. Moritomoto, A. Machida, E. Nishibori, M. Takata, M. Sakata, N. Yamamoto, and H. Takagi, J. Phys. Soc. Jpn. **70**, 1456 (2001).

[66] Y. Horibe, M. Shingu, K. Kurushima, H. Ishibashi, N. Ikeda, K. Kato, Y. Motome, N. Furukawa, S. Mori, and T. Katsufuji, Phys. Rev. Lett. **96**, 086406 (2006); **96**, 169901 (2006).

[67] Y. Shimizu, M. Tanaka, M. Itoh, and T. Katsufuji, Phys. Rev. B **78**, 144423 (2008).

[68] M. Schmidt, W. Ratcliff, P. G. Radaelli, K. Refson, N. M. Harrison, and S. W. Cheong, Phys. Rev. Lett. **92**, 056402 (2004).

[69] P. G. Radaelli, Y. Horibe, M. J. Gutmann, H. Ishibashi, C. H. Chen, R. M. Ibberson, Y. Koyama, Y.-S. Hor, V. Kiryukhin, and S.-W. Cheong, Nature (London) **416**, 155 (2002).

[70] Y. Okamoto, G. J. Nilsen, J. P. Attfield, and Z. Hiroi, Phys. Rev. Lett. **110**, 097203 (2013).